

**Acknowledgments.** The authors wish to express their appreciation to Miss Karin Scheibe for the amino acid analyses and enzymatic analyses and to Miss Roberta

Klimaski for the biological assays. They wish also to thank the Eli Lilly and Co. for a generous gift of crystalline bovine insulin.

## Molecular Interactions in $\beta$ -Lactoglobulin. X. The Stoichiometry of the $\beta$ -Lactoglobulin Mixed Tetramerization<sup>1</sup>

Thomas F. Kumosinski and Serge N. Timasheff

Contribution from the Eastern Regional Research Laboratory,<sup>2</sup> Philadelphia, Pennsylvania 19118. Received June 20, 1966

**Abstract:** The aggregation of  $\beta$ -lactoglobulins A, B, and mixtures of A and B at pH 4.65 has been measured by light scattering and sedimentation. The measurements have been subjected to detailed analysis. The previously postulated stoichiometry, that 30% of the  $\beta$ -lactoglobulin B can form mixed tetramers with 90% of the  $\beta$ -lactoglobulin A, has been discarded. A new, simpler interpretation is based on the assumption that all molecules can aggregate with three types of bonds of different strengths (A-A, B-B, A-B). These three bond types are sufficient to describe quantitatively the progressive tetramerization of mixed lactoglobulins, which can involve fifteen different aggregated species.

In previous communications<sup>3-5</sup> it has been reported that at low temperatures  $\beta$ -lactoglobulin A ( $\beta$ -A) undergoes a reversible tetramerization (from a 36,000 Dalton isoelectric unit to one of 144,000<sup>6</sup>) between pH 3.7 and 5.2 with 90% of the total protein capable of aggregation.<sup>10</sup> The tetramer formed was found to be a closed structure with 422 symmetry.<sup>11,12</sup> The values of the thermodynamic parameters are all negative.<sup>8</sup> The entropy and enthalpy differences become less negative as the pH is increased while the change in free energy passes through a maximum at pH 4.4-4.7.<sup>3,4</sup>

Light scattering and sedimentation data on mixtures of  $\beta$ -A and  $\beta$ -B were interpretable in terms of a stoichiometry in which 30% of the  $\beta$ -lactoglobulin B ( $\beta$ -B) could form mixed tetramers with 90% of the  $\beta$ -A<sup>3,4</sup> while, by itself,  $\beta$ -B could form aggregates no larger than dimers. This interpretation implied that  $\beta$ -A

and  $\beta$ -B have the same specific bonding in the aggregation reaction. The aforementioned conclusion was based upon the observed unimodal sedimentation pattern with the B variant under aggregating conditions,<sup>13</sup> while in the case of  $\beta$ -A a bimodal pattern is observed. Gilbert,<sup>14</sup> in his earlier publications, had concluded that in aggregating systems bimodality could be observed in moving boundary experiments only if the degree of aggregation was to species greater than a dimer, while monomer-dimer equilibrium resulted in a single peak. It was assumed, therefore, that in the case of  $\beta$ -B, the formation of aggregates greater than a dimer was excluded; in  $\beta$ -A- $\beta$ -B mixtures, however, the formation of mixed tetramers was necessary to account both for the light scattering and sedimentation results.<sup>3,10</sup> While this mechanism described in a quantitatively acceptable manner the light scattering data for a variety of  $\beta$ -A- $\beta$ -B mixtures, the stoichiometry was rather cumbersome.

Recently, Gilbert<sup>15</sup> has shown that when aggregation is weak, the hydrodynamic concentration-dependent retardation of moving boundaries assumes major proportions and may overwhelm the bimodality of a reaction boundary, vitiating our previous reasons for limiting the aggregation of  $\beta$ -B to the dimer state. Also, it was found that a hypothetical 30% dimerization of  $\beta$ -B, in the absence of  $\beta$ -A, using the same change in free energy as an (A-A) bond, could not account for recent light scattering (Figure 2) and sedimentation velocity (Figure 7) results. It was then decided that the problem should be reexamined in terms of an alternate stoichiometry, not restricted to a dimerization model. The most reasonable mechanism was found to be one which permitted both genetic variants (A and B) to undergo the tetramerization with different bond strengths, and which abandoned the concept of heterogeneity of the genetic variants with respect to this

(1) This work was presented in part at the 150th National Meeting of the American Chemical Society, Atlantic City, N. J., Sept 1965.

(2) Eastern Utilization Research and Development Division, Agricultural Research Service, U. S. Department of Agriculture.

(3) R. Townend and S. N. Timasheff, *J. Am. Chem. Soc.*, **82**, 3168 (1960).

(4) S. N. Timasheff and R. Townend, *ibid.*, **83**, 464 (1961).

(5) T. T. Herskovits, R. Townend, and S. N. Timasheff, *ibid.*, **86**, 4445 (1964).

(6) In actuality the 36,000-Dalton isoelectric unit is a dimer of two identical chains held together by strong noncovalent bonds.<sup>7</sup> Under the conditions treated here, this dimer undergoes a tetramerization reaction to the 144,000-Dalton octamer; this reaction will be referred to as tetramerization. For purposes of treating the association reaction discussed in this paper, the pertinent kinetic units will be referred to as monomer, dimer, trimer, and tetramer, keeping in mind that they are composed of two, four, six, and eight chains,<sup>7</sup> respectively, with molecular weights of 36,000, 72,000, 108,000, and 144,000. Even though the true chemical subunit is a single chain of 18,000 molecular weight,<sup>8,9</sup> the present usage seems justified, since, under the experimental conditions of this paper, the 36,000-Dalton unit does not dissociate into its two identical subunits.

(7) R. Townend, L. Weinberger, and S. N. Timasheff, *J. Am. Chem. Soc.*, **82**, 3175 (1960).

(8) R. Townend, C. A. Kiddy, and S. N. Timasheff, *ibid.*, **83**, 1419 (1961).

(9) R. Townend, *Arch. Biochem. Biophys.*, **109**, 1 (1965).

(10) R. Townend, R. J. Winterbottom, and S. N. Timasheff, *J. Am. Chem. Soc.*, **82**, 3161 (1960).

(11) J. Wiltz, S. N. Timasheff, and V. Luzzati, *ibid.*, **86**, 168 (1964).

(12) S. N. Timasheff and R. Townend, *Nature*, **203**, 517 (1964).

(13) S. N. Timasheff and R. Townend, *J. Am. Chem. Soc.*, **80**, 4433 (1958).

(14) G. A. Gilbert, *Discussions Faraday Soc.*, No. 20, 68 (1955).

(15) G. A. Gilbert, *Proc. Roy. Soc. (London)*, **A276**, 354 (1963).

reaction.<sup>16</sup> For this purpose more highly precise light scattering and sedimentation experiments were carried out on  $\beta$ -A,  $\beta$ -B, and  $\beta$ -A- $\beta$ -B mixtures of various compositions. These results and their analysis in terms of the new stoichiometry are presented in this publication.

## Experimental Section

**Materials and Methods.** The genetic variants of  $\beta$ -lactoglobulin ( $\beta$ -A and  $\beta$ -B) were prepared from the milk of homozygous cows by the method of Aschaffenburg and Drewry.<sup>21</sup> Mixtures of various compositions were prepared by mixing analyzed solutions of pure  $\beta$ -A with solutions of pure  $\beta$ -B in known amounts. Each protein was freshly recrystallized immediately prior to the experiments.

The light-scattering measurements were carried out at 436 m $\mu$  in the Brice<sup>22</sup> photometer using 2-mm slit optics. Stock solutions of the pure genetic variants were made up in acetate buffer (pH 4.65,  $\Gamma/2 = 0.1$ ) and dialyzed overnight vs. a large excess of the buffer. The solutions were then clarified in a Spinco Model L centrifuge<sup>23</sup> and their concentrations were measured by ultraviolet absorption at 278 m $\mu$  using a value of 0.96 l./g for the absorptivity.<sup>10</sup> At this point the various mixtures were prepared by volumetric procedures. The stock mixtures were then filtered through an ultrafine sintered-glass filter of special design.<sup>24,25</sup> The working solutions were made up by dilution into Dintzis-type cells<sup>26</sup> using an ultramicro buret. The solvent scattering of each cell was measured before adding the protein.

Temperature control was attained by placing the filled cells into a constant-temperature water bath. All solutions were prepared and first measured at 25°, and the temperatures of the water bath and the room were then decreased progressively for the successive sets of measurements. This order minimized leakage out of the cell caused by air expansion, which occurs often if the temperature is raised. The concentrations of the solutions in each cell were verified after each run in order to rule out evaporation or leakage.

Ultracentrifugal experiments were carried out in a Spinco Model E analytical ultracentrifuge<sup>23</sup> at 59,780 rpm, using Kel-F cells. Runs were controlled at 25 and 2°.

**Calculations.** All light-scattering data were treated in terms of the reduced three component light-scattering equation<sup>26-29</sup> (eq 1), since it had been shown previously<sup>3</sup> that the contribution of protein-buffer interactions to the scattering in this case is smaller than experimental error and can be neglected.

$$\frac{HC_2}{\Delta\tau} = \frac{1}{\bar{M}_w} + \frac{2B_0C_2}{M_m} \quad (1)$$

(16) It is of interest to point out that neither the known third genetic variant of bovine  $\beta$ -lactoglobulin ( $\beta$ -C),<sup>17</sup> which differs from  $\beta$ -B by the substitution of a single amino acid,<sup>18</sup> nor goat  $\beta$ -lactoglobulin, which differs from  $\beta$ -B by three amino acids,<sup>19</sup> nor sheep  $\beta$ -lactoglobulin<sup>20</sup> can participate in this reaction to any detectable degree. It is also noteworthy that all three variants— $\beta$ -lactoglobulin C, goat and sheep  $\beta$ -lactoglobulin—have the same amount of aspartic acid as (or less than)  $\beta$ -lactoglobulin B.<sup>18-20</sup>

(17) R. Townend, T. T. Herskovits, H. E. Swaisgood, and S. N. Timasheff, *J. Biol. Chem.*, **239**, 4196 (1964).

(18) E. B. Kalan, R. Greenberg, M. Walter, and W. G. Gordon, *Biochem. Biophys. Res. Commun.*, **16**, 199 (1964).

(19) R. Townend, manuscript in preparation.

(20) J. L. Maubois, R. Pion, and B. Ribadeau-Dumas, *Biochim. Biophys. Acta*, **107**, 501 (1965).

(21) R. Aschaffenburg and J. Drewry, *Biochem. J.*, **65**, 273 (1957).

(22) B. A. Brice, M. Halwer, and R. Speiser, *J. Opt. Soc. Am.*, **40**, 768 (1950).

(23) Mention of specific firms and products does not imply endorsement by the U. S. Department of Agriculture to the possible detriment of others not mentioned.

(24) F. F. Nord, M. Bier, and S. N. Timasheff, *J. Am. Chem. Soc.*, **73**, 289 (1951).

(25) M. Bier, *Methods Enzymol.*, **4**, 165 (1957).

(26) S. N. Timasheff, H. M. Dintzis, J. G. Kirkwood, and B. D. Coleman, *J. Am. Chem. Soc.*, **79**, 782 (1957).

(27) J. G. Kirkwood and R. J. Goldberg, *J. Chem. Phys.*, **18**, 54 (1950).

(28) W. H. Stockmayer, *ibid.*, **18**, 58 (1950).

(29) H. C. Brinkman and J. J. Hermans, *ibid.*, **17**, 574 (1949).

where

$$H = \frac{32\pi n^2(\delta n/\delta C_2)^2}{3\lambda^4 N}$$

$\Delta\tau$  is the excess turbidity over solvent scattering,  $C_2$  the total protein concentration in g/l.,  $\bar{M}_w$  the weight-average molecular weight of the system,  $B_0$  the second virial coefficient of the monomer whose value was taken as  $0.9 \times 10^{-8}$  l. g<sup>-1</sup>,<sup>11</sup>  $n$  the refractive index of the solvent,  $\lambda$  the wavelength of the light in cm, and  $N$  Avogadro's number. The term  $M_m$  is the monomer molecular weight and was obtained for each run from the intercept of the  $HC_2/\Delta\tau$  vs.  $C_2$  plot.

All calculations were made on an IBM-1620 Model II computer using two Fortran programs developed by T. F. K.

## Results

The light-scattering experiments (Figures 1-5), performed on  $\beta$ -A,  $\beta$ -B, and mixtures of the two variants, were carried out in  $\Gamma/2 = 0.1$  acetate buffer, pH 4.65, and temperatures of 25, 15, 8, 4.5, and 2°.

The light-scattering data on  $\beta$ -A (Figure 1) show an increase of turbidity with an increase in concentration, which indicates strong attraction between protein molecules and can be interpreted in terms of normal mass-action aggregation. This aggregation increases with decreasing temperature; the effect is obtained also with  $\beta$ -B (Figure 2) but not as markedly as with  $\beta$ -A. The shape of the  $\beta$ -A (Figure 1) scattering curve at 25° is similar to the corresponding  $\beta$ -B curve (Figure 2) at 4.5°. This may be a further indication that the  $\beta$ -B reaction involves the same type of aggregates as the  $\beta$ -A reaction but that the relative amounts differ at any one temperature.

Observation of the scattering of various  $\beta$ -(A-B) mixtures (Figures 3-5) reveals a monotonic increase in the weight-average molecular weight,  $\bar{M}_w$ , as the fraction of  $\beta$ -A is increased. At a constant total concentration of 20 g/l. and at a temperature of 2°, the  $\bar{M}_w$  at a composition of zero  $\beta$ -A (pure  $\beta$ -B) is 48,000 Daltons. At 15.6, 32.0, and 52.0%  $\beta$ -A,  $\bar{M}_w$  is 71,700, 92,500, and 110,000, respectively. For pure  $\beta$ -A,  $\bar{M}_w$  is 131,300. This effect of composition is seen more easily in Figure 6, where the weight-average molecular weights obtained from light scattering at 2° using these compositions are compared. It seems also significant that the relative curvatures of the various curves (Figure 6) are similar. This is consistent again with the concept that the type of aggregates is the same and that only their relative amounts differ.

Sedimentation results on  $\beta$ -B (Figure 7) show a small increase in sedimentation coefficient,  $s_{20,w}$ , with a decrease in temperature. At a concentration of 58 g/l. the  $s_{20,w}$  at 25° is 2.01 S while at 2° this value becomes 2.47 S. While this increase indicates the presence of aggregated molecular species, it cannot be compared directly to the light-scattering results on  $\beta$ -B (Figure 2) without taking into account the large retardation of sedimentation due to the hydrodynamic drag of the various sedimenting species at these concentrations.

## Discussion

**Stoichiometry of Tetramerization.** In previous communications, the light-scattering data on pure  $\beta$ -A were treated in terms of a simple monomer-tetramer model.<sup>3,4</sup> Theoretical curves for such a stoichiometry at 15 and 8° were calculated using previously reported equilibrium constants and assuming that all the mole-

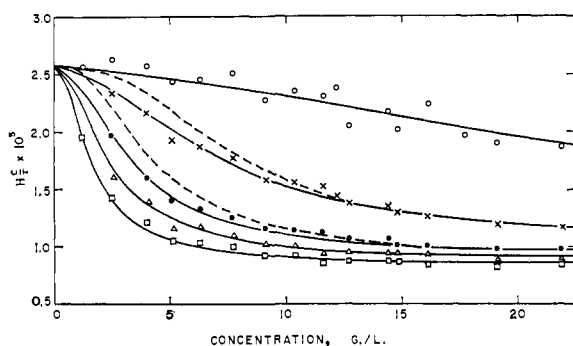


Figure 1. Light-scattering data on  $\beta$ -lactoglobulin A in 0.1 ionic strength acetate buffer, pH 4.65; O, 25°; X, 15°; ●, 8°;  $\Delta$ , 4.5°;  $\square$ , 2°; —, theoretical curve for progressive tetramerization model at indicated temperatures; - - -, theoretical curve for simple monomer-tetramer model at 15 and 8°.

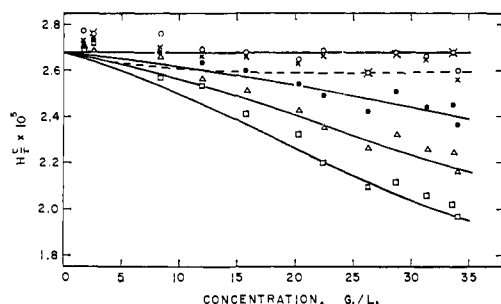


Figure 2. Light scattering data on  $\beta$ -lactoglobulin B in 0.1 ionic strength acetate buffer, pH 4.65. Symbols have same meaning as in Figure 1. Dashed line is the theoretical curve for the dimerization of 30% of  $\beta$ -B at 2°.

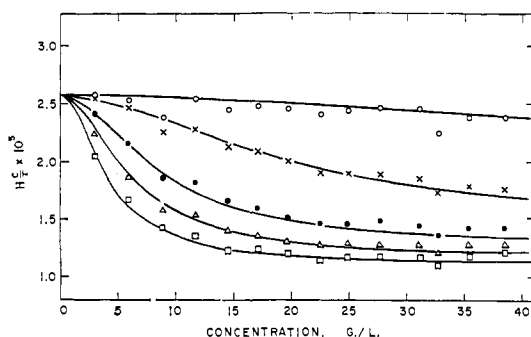


Figure 3. Light-scattering data on  $\beta$ -lactoglobulin (A-B) mixture containing 32.0%  $\beta$ -A in 0.1 ionic strength acetate buffer, pH 4.65. Symbols have same meaning as in Figure 1. Solid lines are the best theoretical curves for a progressive mixed tetramerization model.

cules of  $\beta$ -A are equally capable of aggregation; these curves are represented by the dashed lines of Figure 1. Since the agreement is rather poor in the low concentration range (below 7 g/l.), a progressive tetramerization (monomer  $\rightarrow$  dimer  $\rightarrow$  trimer  $\rightarrow$  tetramer) model was examined. It had been found previously<sup>4</sup> that such a model describes the  $\beta$ -A data at 4.5° as satisfactorily as the simple monomer-tetramer equilibrium. In this model, if it is assumed that the energies of all four intermolecular bonds are identical, with only a statistical factor intervening in the last step, it is easily shown from the law of mass action that the total concentra-

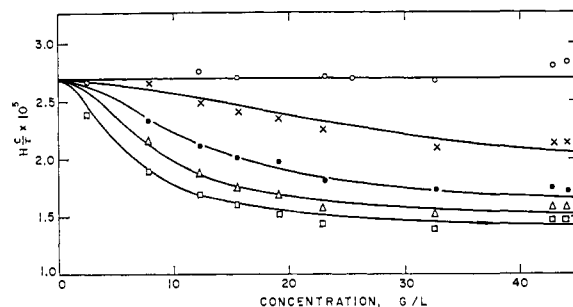


Figure 4. Light-scattering data on  $\beta$ -lactoglobulin (A-B) mixture containing 15.6%  $\beta$ -A in 0.1 ionic strength acetate buffer, pH 4.65. Symbols have same meaning as in Figure 1. Solid lines are the best theoretical curves for a progressive mixed tetramerization model.

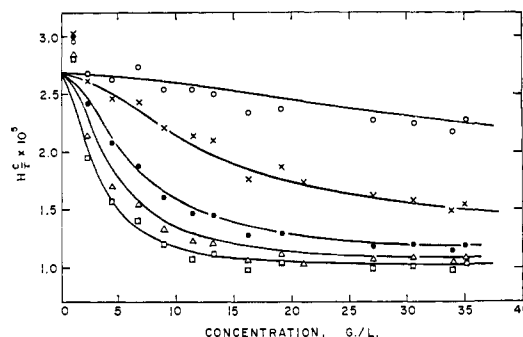


Figure 5. Light-scattering data on  $\beta$ -lactoglobulin (A-B) mixture containing 52.0%  $\beta$ -A in 0.1 ionic strength acetate buffer, pH 4.65. Symbols have same meaning as in Figure 1. Solid lines are the best theoretical curves for a progressive mixed tetramerization model.

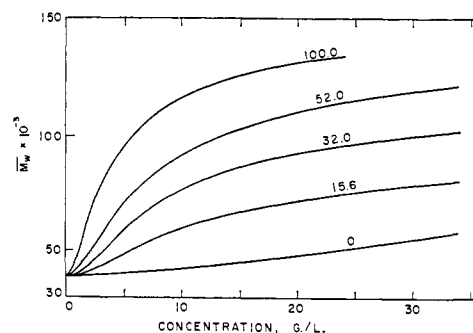


Figure 6. Comparison of the weight-average molecular weights of various fractions of  $\beta$ -(A-B) mixtures at 2° from theoretical light-scattering curves in Figures 1-5. The fractions of  $\beta$ -A for the curves are marked on the figure as weight per cent of  $\beta$ -A.

tion,  $C_2$ , in g/l., is related to the aggregates present by

$$C_2 = M_m \sum_{n=1}^4 n\gamma(k_i)^{n-1} A^n \quad (2)$$

where

$$\gamma = \begin{cases} 1 & n = 1-3 \\ k_{i/4} & n = 4 \end{cases}$$

$A$  is the concentration of the monomer species in moles per liter,  $n$  is the degree of aggregation,  $M_m$  is the monomer molecular weight and  $k_i$  is the equilibrium constant for the formation of an intermolecular bond; here  $k_i$  will be defined as the constant for the formation

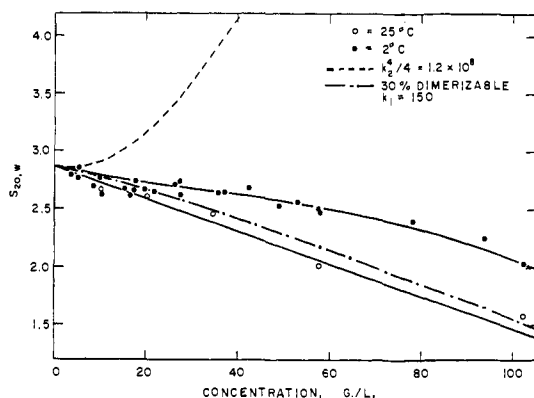


Figure 7. Sedimentation velocity data on  $\beta$ -lactoglobulin B in 0.1 ionic strength acetate buffer, pH 4.65: O, 25°; ●, 2°; (upper —), theoretical for progressive tetramerization model with hydrodynamic effect using equilibrium constant obtained from light-scattering data at 2°; (lower —), least-squares line for obtaining the hydrodynamic factor "g"; - - - - -, theoretical curve for 30% dimerizable model using the same equilibrium constant as  $\beta$ -lactoglobulin A; ·····, theoretical curve for simple monomer-tetramer equilibrium without hydrodynamic retardation.

of an A-A bond,  $k_1$ .<sup>30</sup> The weight-average molecular weight,  $\bar{M}_w$ , is then given by

$$\bar{M}_w = \frac{M_m \sum_{n=1}^4 n^2 \gamma(k_i)^{n-1} A^n}{\sum_{n=1}^4 n \gamma(k_i)^{n-1} A^n} \quad (3)$$

Using the equations (1-3), values of  $k_1$  were deduced from the experimental data at each temperature, and the best theoretical curves for the progressive tetramerization model based on these values were constructed; these are represented by the solid lines in Figure 1. The agreement is excellent at all temperatures and concentrations. It should be noted, however, that progressive tetramerization makes a significant contribution only at concentrations less than 15 g/l. and at temperatures between 4.5 and 25°. Therefore, the simple monomer-tetramer model for  $\beta$ -A is a good approximation at concentrations greater than 15 g/l. as well as at temperatures close to 0°. While it has been shown previously that at 4.5° intermediate aggregates are present in negligible amounts relative to monomer and tetramer,<sup>4</sup> the situation is quite different at intermediate temperatures, as is shown in Figure 8, where the per cent contribution of monomer, dimer, trimer, and tetramer is plotted as a function of total concentration at 8°.

The light scattering of  $\beta$ -B was also fitted in similar manner to a progressive tetramerization model. The results are shown in Figure 2. The agreement is again very good. New values of the bond formation equilibrium constant,  $k_i$ , were determined at each tempera-

(30) It should be noted that in the present analysis the four intermolecular bonds are regarded as being equivalent, with only a statistical factor of  $1/4$  introduced in the formation of the fourth bond which involves closing of the ring. While, mechanistically, the free energy of formation of the fourth bond may differ significantly from that of the first three, due to the entropic effects involved in the closing of the ring, intrinsically the bonds are identical and may be treated as such in the present thermodynamic analysis. Furthermore, the fact that the formation of intermediate dimer and trimer species (with one bond and two bonds, respectively) can be described reasonably in terms of the above treatment indicates that the free energy of formation of the fourth bond is indeed similar to that of the first three within the statistical factor of  $1/4$ .

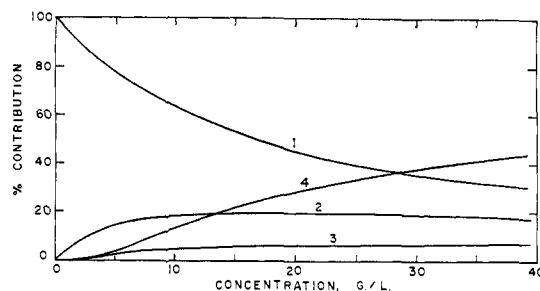


Figure 8. Per cent contribution of each species to the total concentration as a function of  $\beta$ -lactoglobulin concentration for the progressive tetramerization of  $\beta$ -lactoglobulin A in 0.1 ionic strength acetate buffer, pH 4.65 and 8°: 1, monomer contribution; 2, dimer contribution; 3, trimer contribution; 4, tetramer contribution.

ture. These parameters are defined as  $k_2$  for  $\beta$ -B and are a measure of the energy of a bond between two  $\beta$ -B molecules. The values of  $k_1$  and  $k_2$  obtained in this manner are summarized in Table I.

Table I. Thermodynamic Parameters of  $\beta$ -Lactoglobulin (A-B) Aggregation

Temp, °C	$k_1$	$-\Delta F_1$ , kcal	$k_2$	$-\Delta F_2$ , kcal	$k_3$	$-\Delta F_3$ , kcal
25	196.0	3.13	20.7	...	125.0	(2.86)
15	487.0	3.54	46.3	...	342.0	(3.34)
8	865.0	3.78	85.1	2.48	686.0	3.65
4.5	1106.0	3.86	116.0	2.62	952.0	3.78
2	1500.0	4.00	146.0	2.72	1300.0	3.92
		$\Delta H_1 = -13.7$		$\Delta H_2 = -13.8$		$\Delta H_3 = -14.5$
		kcal		kcal		kcal
	$\Delta S_{av} = -35.4$		$\Delta S_{av} = -40.3$		$\Delta S_{av} = -38.6$	
	eu		eu		eu	

In order to check the validity of the previously assumed stoichiometry which stated that only 30% of  $\beta$ -B can form mixed tetramers with  $\beta$ -A or dimerize in pure form, a theoretical curve for the scattering of  $\beta$ -B in which only 30% could dimerize with the same free-energy change as an A-A bond (corresponding to  $k_1$ ) was calculated for the reaction at 2°. This curve is depicted in Figure 2 by the dotted line. The agreement is seen to be quite poor. This result weakens but does not totally disprove the old stoichiometry, since such a disagreement could conceivably be the result of unusually large negative virial coefficients in  $\beta$ -B, while  $\beta$ -A exhibits the expected small positive virial coefficient.

In order to arrive at an unequivocal choice between the stoichiometries, sedimentation data obtained with  $\beta$ -B at 25 and 2° were fitted to these models in the following manner.

Since light-scattering results showed conclusively that  $\beta$ -B exists only as a monomer at 25° (Figure 2), sedimentation data on  $\beta$ -B at 25° were used to calculate the hydrodynamic factor,  $g$ , defined by Gilbert<sup>15</sup> as

$$s = s_1(1 - gC_2) \quad (4)$$

where  $s_1$  is the sedimentation coefficient of the monomer at infinite dilution,  $s$  is the sedimentation coefficient at the leading edge of the boundary, and  $C_2$  is the total protein concentration in g/l. The 25° data, shown in Figure 7, result in a value of  $g = 0.00494$  l./g.

The expected sedimentation coefficients for the progressive tetramerization and the 30% dimerization models were then calculated according to Gilbert<sup>15</sup>

$$s = \frac{\sum_{n=1}^j n\gamma_j s_n (k_j)^{n-1} B^n}{\sum_{n=1}^j n\gamma_j (k_j)^{n-1} B^n} (1 - gC_2) \quad (4a)$$

where  $s_n$ 's are the sedimentation coefficients of the individual aggregates, which have been calculated from our earlier data<sup>4,10</sup> ( $s_1 = 2.87$ ,  $s_2 = 4.56$ ,  $s_3 = 6.08$ ,  $s_4 = 7.38$ );  $j = 4$  for the progressive tetramerization model and  $j = 2$  for the 30% dimerization model

$$\gamma_j = \begin{cases} 1 & j = 2 \\ 1 & j = 4, n = 1-3 \\ k_{2/4} & j = 4, n = 4 \end{cases} \quad (4b)$$

$$k_j = \begin{cases} k_1 (\text{A-A bond}), & j = 2 \\ k_2 (\text{B-B bond}), & j = 4 \end{cases} \quad (4c)$$

and  $B$  is the monomer concentration in moles/l.

In these sedimentation experiments, the stoichiometric concentration,  $C^*$ , which is represented by

$$C^* = M_m \sum_{n=1}^j n\gamma_j (k_j)^{n-1} B^n \quad (5)$$

is not equal to the total protein concentration,  $C_2$ , because the sedimentation patterns were not calculated by the usual second moment technique.<sup>31</sup> Only in a nonaggregating, ultracentrifugally homogeneous system is  $C^*$  approximately equal to the total protein concentration (see eq 4). It has been shown, however, that the total protein concentration is related in a simple manner to the stoichiometric concentration in an aggregating system.<sup>15,32</sup>

Results of calculations with eq 4 using the 30% dimerization model and light-scattering values of  $k_1$  are represented by the dot-dashed line in Figure 7; this gives a rather poor fit to the 2° data, while similar calculations with the progressive tetramerization model, represented by the solid line in Figure 7, give excellent agreement. It can be concluded, therefore, that the 30% dimerization model is a highly unlikely representation of the observed aggregation and that the progressive tetramerization model is the correct interpretation of the observations.

The magnitude of the hydrodynamic drag is clearly evident from Figure 7 in which the dashed line is a theoretical curve calculated for a simple monomer-tetramer model with neglect of the hydrodynamic retardation. This curve was calculated according to Gilbert<sup>14</sup> by the following

$$C^* = \left( \frac{k_2 \delta}{161 - \delta} \right)^{1/3} \left( 1 + \frac{1}{4} \frac{\delta}{1 - \delta} \right) \quad (6a)$$

where  $C^*$  is again the stoichiometric concentration, proportional to the total protein concentration in g/l.;<sup>15,32</sup> and

$$\delta = \frac{s - s_1}{s_4 - s_1} \quad (6b)$$

A simultaneous solution of eq 6a and b gives the

(31) R. J. Goldberg, *J. Phys. Chem.*, **57**, 194 (1953).  
 (32) G. A. Gilbert, private communications.

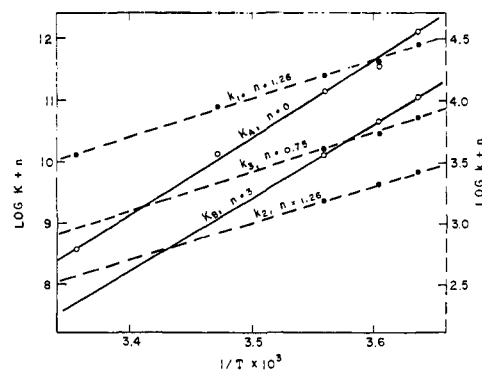


Figure 9. van't Hoff plots for  $\beta$ -lactoglobulin progressive tetramerization from light-scattering data:  $\circ$ , 100%  $\beta$ -A ( $K_A$ ) and 100%  $\beta$ -B ( $K_B$ ), respectively;  $\bullet$ , equilibrium constants of A-A ( $k_1$ ), B-B ( $k_2$ ), and A-B ( $k_3$ ) bonds. To prevent overlap, the plots have been mutually displaced by arbitrary constants,  $n$ , shown on the figure for each curve. Solid lines refer to left ordinate, dashed lines to right ordinate.

desired monomer-tetramer theoretical curve. Comparison of the progressive tetramerization with hydrodynamics accounted for (solid line of Figure 7) and the simple monomer-tetramer curves (dashed line of Figure 7) clearly shows the overpowering effect of hydrodynamic retardation on a weak association. In this case, the normally observed rapidly sedimenting peak is actually pushed back into the slow monomer peak. In this weakly aggregating system, the Gilbert  $C_{\min}$ <sup>33</sup> is extremely large and the expected bimodality never develops as the two peaks are hydrodynamically merged into one (eq 4a).

With the validation of the stoichiometry of the  $\beta$ -A and  $\beta$ -B aggregation, the thermodynamic parameters for formation of the low-temperature octamer from the dimer were calculated from the light-scattering data by the following

$$\Delta F^\circ = -RT \ln K_a \quad (7a)$$

where  $\Delta F^\circ$  is the standard free-energy change of the  $4\beta \rightleftharpoons \beta_4$  reaction,  $R$  the gas constant,  $T$  the thermodynamic temperature, and  $K_a$  the equilibrium constant of the reaction which is equal to  $k_1^4/4$  or  $k_2^4/4$  for  $\beta$ -A or  $\beta$ -B, respectively.

$$\Delta H^\circ = -\frac{1}{R} \frac{d \ln K_a}{d(1/T)} \quad (7b)$$

where  $\Delta H^\circ$  is the change in enthalpy; and

$$\Delta S^\circ = \frac{\Delta H^\circ - \Delta F^\circ}{T} \quad (7c)$$

where  $\Delta S^\circ$  is the change in entropy of the reaction.

van't Hoff plots of the  $\beta$ -A and  $\beta$ -B data for the calculation of  $\Delta H^\circ$  are shown in Figure 9; it is evident that the two sets of points fall on parallel straight lines. This would indicate that the enthalpy changes of the  $\beta$ -A and  $\beta$ -B reactions are essentially the same. The values of the thermodynamic parameters calculated in this manner are listed in Table II. Inspection shows that the free energy of the  $\beta$ -B reaction at a given temperature is less than that of the  $\beta$ -A reaction, a result which was clearly expected. Although the

(33)  $C_{\min}$  is defined<sup>14</sup> as the concentration above which the rapid peak starts to appear in the absence of hydrodynamic retardation.<sup>15</sup>

**Table II.** Thermodynamic Parameters of  $\beta$ -Lactoglobulin Homologous Tetramerization

Temp, °C	$4A \rightleftharpoons A_4$		$4B \rightleftharpoons B_4$	
	$-\Delta F,$ kcal	$-\Delta S,$ eu	$-\Delta F,$ kcal	$-\Delta S,$ eu
25	11.69	150.9	...	...
15	13.38	150.3	...	...
8	14.33	150.6	9.15	165.7
4.5	14.70	151.2	9.72	165.8
2	15.23	150.6	10.13	165.8
	$\Delta H = -56.66$ kcal		$\Delta H = -55.72$ kcal	
	$\Delta S_{av} = -150.7$ eu		$\Delta S_{av} = -165.8$ eu	

**Table III.** Molecular Aggregates in  $\beta$ -(A-B) Mixtures

I. Dimers	A-A	B-B	A-B
	$k_1 = \frac{[A-A]}{[A]^2}$	$k_2 = \frac{[B-B]}{[B]^2}$	$k_3 = \frac{[A-B]}{[A][B]}$
II. Trimers	A-A   A	B-B   B	A-B   B
	$k_1^2$	$k_2^2$	$k_3^2$
	B-A   A	B-A   B	A-B   A
	$k_3^2$	$k_2 k_3$	$k_1 k_3$
III. Tetramers	A-A     A-A	B-B     B-B	A-A     A-B
	$k_1^4/4$	$k_2^4/4$	$(k_1 k_3)^2/4$
	A-A     B-B	A-B     B-A	A-B     B-B
	$k_1 k_2 k_3^2/4$	$k_3^4/4$	$(k_2 k_3)^2/4$

enthalpy changes are nearly equal, it should be noted that the corresponding entropy changes differ by 15.1 eu. Comparison of these values with those reported previously<sup>3</sup> using a simple tetramerization (dimer  $\rightarrow$  octamer) equilibrium shows that no drastic revisions in the thermodynamic parameters of  $\beta$ -A tetramer (eight chains) formation are necessary as a result of the new data analysis in terms of the more exact progressive aggregation stoichiometry.

In order to describe the  $\beta$ -(A-B) mixed aggregation, all possible aggregates from dimer to tetramer of the isoelectric two-chain species were expressed in the simplest manner; namely, in terms of three types of bonds, each described by its equilibrium constant— $k_1$  (A-A),  $k_2$  (B-B), and  $k_3$  (A-B). The possible hybrids and their relation to the three bonds are shown in Table III; in all, 15 different aggregated species may exist simultaneously in solution.

With  $k_1$  and  $k_2$  known from the light-scattering experiments on  $\beta$ -A and  $\beta$ -B at each temperature,  $k_3$  had to be derived from experiments on mixtures of known weight fractions of  $\beta$ -A. The complexity of this system results in analytical expressions being obtainable only for the relations between monomer concentration and total concentration,  $C_2$ , weight-average molecular weight,  $\bar{M}_w$ , and weight fraction of  $\beta$ -A (fraction A). The corresponding functions are

$$\bar{M}_w = \frac{M_m \left[ \sum_{n=1}^4 n^2 \gamma_1 (k_1)^{n-1} A^n + \sum_{r=1}^4 r^2 \gamma_2 (k_2)^{r-1} B^r + \sum_{n=1}^3 \sum_{r=1}^3 (n+r)^2 \gamma_{nr} A^n B^r \right]}{C_2} \quad (8a)$$

fraction A =

$$\frac{M_m \left[ \sum_{n=1}^4 n^2 \gamma_1 (k_1)^{n-1} A^n + \sum_{n=1}^3 \sum_{r=1}^3 n \gamma_{nr} A^n B^r \right]}{C_2} \quad (8b)$$

and

$$C_2 = M_m \left[ \sum_{n=1}^4 n \gamma_1 (k_1)^{n-1} A^n + \sum_{r=1}^4 r \gamma_2 (k_2)^{r-1} B^r + \sum_{n=1}^3 \sum_{r=1}^3 (n+r) \gamma_{nr} A^n B^r \right] \quad (8c)$$

where

$$\gamma_1 = \begin{cases} 1 & n=1-3 \\ k_1/4 & n=4 \end{cases} \quad (8d)$$

$$\gamma_2 = \begin{cases} 1 & n=1-3 \\ k_2/4 & n=4 \end{cases} \quad (8e)$$

$$\gamma_{nr} = \begin{pmatrix} k_3 & k_3^2 + k_2 k_3 & \frac{(k_2 k_3)^2}{4} \\ k_3^2 + k_1 k_3 & \frac{k_3^2 (k_3^2 + k_1 k_2)}{4} & 0 \\ \frac{(k_1 k_3)^2}{4} & 0 & 0 \end{pmatrix} \quad (8f)$$

A and B are the concentrations of the  $\beta$ -A and  $\beta$ -B monomer species in moles/l., and  $k_1$ ,  $k_2$ , and  $k_3$  are the equilibrium constants of A-A, B-B, and A-B bond formation.

At any given weight fraction of  $\beta$ -A, the above equations can be solved simultaneously using a numerical method. A Fortran program has been developed by which  $k_3$  can be determined, given the values of  $k_1$ ,  $k_2$ , and the scattering data at a given fraction A. Using the  $k_1$  and  $k_2$  values obtained from the experiments with pure  $\beta$ -A and  $\beta$ -B (Table I), the values of  $k_3$  at the indicated temperatures were calculated from the light-scattering data on an A-B mixture having 32.0%  $\beta$ -A (Figure 3).

Using these derived values of  $k_1$ ,  $k_2$ , and  $k_3$ , theoretical curves for light scattering at a fraction of  $\beta$ -A of 15.6% (Figure 4) and 52.0% (Figure 5) were calculated with eq 8a-f using another Fortran program and compared with the experimental data at these compositions. The agreement between the theoretical curves (the solid lines of Figures 4 and 5) and the light-scattering experimental points is excellent at both compositions. Hence, the stoichiometry of the  $\beta$ -(A-B) mixed interaction with the participation of all protein molecules present in solution is established and the old 30% aggregable model must be discarded. This stoichiometry is quite dependent upon the fraction of  $\beta$ -A in the mixture. Figure 6 shows the theoretical scattering at 2° as a function of the fraction of  $\beta$ -A, represented as weight-average molecular weight. For example, at a protein concentration of 20 g/l. the weight-average molecular weight increases by 49.4% when the fraction of A changes from 0 to 15.6%, while only a 29.0% increase is observed when the fraction of A increases from 15.6 to 31.8%. This behavior is a further indication of the presence of intermediate aggregates in the mixture, while the overall increase in the scattering as a function of the fraction of  $\beta$ -A is additional qualitative verification of the

existence of mixed tetramers with bonds of different strengths.

The thermodynamic parameters of the A-A ( $k_1$ ), B-B ( $k_2$ ), and A-B ( $k_3$ ) bonds were calculated from eq 7a-c and the results are shown in Table I. The enthalpy changes were calculated from the van't Hoff plots shown in Figure 9 and the values of  $\Delta H^\circ$  for the A-A, B-B, and A-B interactions were found to be identical within experimental error. The free-energy change of the B-B bond is less than that of the A-B bond, while the entropy change of the A-B bond is intermediate between the two homologous bonds and is slightly less negative than that of the B-B bond. The A-A bond has the largest change in free energy and the smallest entropy change. Thus the difference between the free energies of tetramer formation of  $\beta$ -A and  $\beta$ -B is a reflection of a slightly larger decrease in entropy which accompanies the aggregation of  $\beta$ -B. Since the stoichiometries and, hence, the geometries of formation of the eight-sphere tetramer<sup>11,12</sup> from the two-sphere units are identical in the two genetic variants, it can be expected that the loss of over-all configurational entropy due to the mutual immobilization of four units is identical for the two proteins. The observed difference in entropy must reflect then a difference in the actual A-A, A-B, and B-B intermolecular bonds formed. It is known that, in the tetramerization of  $\beta$ -A, four carboxyls per polypeptide chain are protonated;<sup>8,4</sup> it has been suggested<sup>9,35</sup> that one of these carboxyls is the difference aspartic acid residue in the sequence of  $\beta$ -A, which is genetically substituted for a glycine residue in  $\beta$ -B.<sup>9</sup> It is quite possible that the smaller decrease in entropy in the case of  $\beta$ -A reflects the release of a larger number of water molecules as the carboxyls are transported into the hydrophobic interior of the tetramer. This lesser loss in entropy, in turn, would result in the greater free energy of the association of  $\beta$ -A. Such phenomena could exemplify the major changes in the solution properties of a protein which can be introduced by a single amino acid substitution.

**Heterogeneity of  $\beta$ -Lactoglobulin A.** The above calculations have been based upon the premise that 100% of the protein can react both in the case of  $\beta$ -A and  $\beta$ -B. In the present experiments it was not found necessary to invoke the previously observed 10% of inert species<sup>7,10,36</sup> in  $\beta$ -A. As a result, sedimentation experiments were devised to test the purity of the  $\beta$ -A preparations used in these and past experiments.

Gilbert<sup>14</sup> has stated that in a simple monomer-tetramer equilibrium, the area of the slow peak remains constant with concentration after attainment of the concentration<sup>38</sup> at which the rapid peak first appears. This area is a function of the size of the aggregates and of the equilibrium constant. Therefore, above this concentration and at a constant temperature the area of the slow peak should change only if an impurity is present. Any excess area in the slow peak (area > the predicted Gilbert slow peak area) is proportional to the amount of inert material present (assuming, of course, that the  $s_{20,w}$  of the inert material is not too different from that of the monomer).

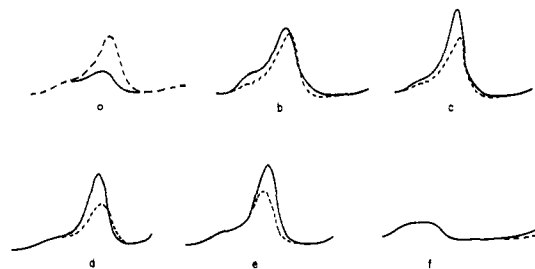


Figure 10. Sedimentation patterns of  $\beta$ -lactoglobulin A samples in 0.1 ionic strength acetate buffer at pH 4.65, 2°: a, —, new preparation, 5.9 g/l.; —, new preparation, 11.9 g/l.; b-e, —, new preparation,  $C = 11.9$  g/l.; - - - -, b, Aschaffenburg preparation,  $C = 17.7$  g/l.; c, Cow No. 3495 preparation,  $C = 17.4$  g/l.; d, new preparation at room temperature for 3 days,  $C = 17.0$  g/l.; e, new preparation in contact with toluene for 6 years,  $C = 19.3$  g/l.; f, —, new preparation,  $C = 3.0$  g/l.; - - - -, supernatant from recrystallization of new preparation,  $C = 4.0$  g/l. All times and bar angles are the same within each pair of patterns.

Schlieren patterns showing the two cases are presented in Figure 10.

Figure 10a shows the sample used in this study. It is evident that the area under the slow peak remains constant when the total concentration is increased by a factor of 3. Thus, the  $\beta$ -A preparation used here contains no nonaggregable material and can be regarded as homogeneous from the point of view of this reaction. The same is not the case, however, with the material furnished us by Aschaffenburg (pattern b) and the preparation made in our laboratory (pattern c), both of which had been used in the previous aggregation experiments.<sup>3,4,10</sup> The dashed-line patterns in each case were obtained with the 100% aggregable material, while the solid-line patterns represent the earlier preparations. It can be seen that in both cases the areas under the slow peaks are not equal, meaning that some inert material is present. The amount is *ca.* 10% of the total protein in both cases.

In an attempt to explain the presence of the inert protein under seemingly identical conditions of preparation, several control experiments were performed; these were based on the assumption that the inert material was due either to enzymatic degradation of the protein during storage or to interaction of the protein with toluene, since one of these  $\beta$ -lactoglobulin preparations was stored under toluene. That enzymatic degradation does occur with storage of some crystalline samples, even in the presence of toluene, has been shown by Townend<sup>37</sup> who found that high voltage electrophoresis patterns of the mother liquor from crystals of a  $\beta$ -A preparation used in the earlier studies contained bands resembling degradation peptides, even if the protein had been stored in the cold; no such bands were observed immediately after recrystallization. That the preparation used in the present study was not undergoing such degradation is evidenced by ultracentrifugal experiments performed on materials that had been left standing as a crystal slurry for 3 days at room temperature (Figure 10d), as well as the stored supernatant from the recrystallization of this protein (Figure

(34) R. Townend and S. N. Timasheff, manuscript in preparation.

(35) S. N. Timasheff and R. Townend, *J. Dairy Sci.*, **45**, 259 (1962).

(36) M. P. Tombs, *Biochem. J.*, **67**, 517 (1957).

(37) R. Townend, private communication.

10f). In neither case does the area under the slow peak exceed that predicted for 100% aggregation. The hypothesis of interaction with toluene was apparently eliminated in an experiment on a preparation that had been stored unopened for 6 years under toluene. As is evident from Figure 10e, again there is no evidence of inert material under the slow peak. Thus, it would seem that, in some preparations of  $\beta$ -lactoglobulin, a trace amount of proteolytic enzyme has become introduced, with a resulting slow degradation of the protein and its inertness toward the low-temperature tetramerization.

As a final check on the validity of analysis of the previously published data<sup>4</sup> in terms of 10% nonaggregable  $\beta$ -A, these data were analyzed with the present stoichiometry. In all cases, the values of  $k_1$ ,  $k_2$ , and  $k_3$  reported in the present paper, along with an assumption that only 90% of  $\beta$ -A but all of  $\beta$ -B can participate in this reaction, were found to describe the data quantitatively, validating the conclusion that the earlier preparations of  $\beta$ -A were not completely homogeneous.

## Conclusion

The data and the analysis presented here establish a new, simpler, and more reasonable stoichiometry for the low-temperature tetramerization of  $\beta$ -A and  $\beta$ -B, as well as mixtures of the two lactoglobulins from isoelectric dimers to the low-temperature octamer. The old stoichiometry,<sup>4,6</sup> which consisted of constant bond strengths and certain proportions of unaggregable material, is hereby withdrawn as unrealistic. The new interpretation proposes bonds of three different strengths, namely, an A-A, a B-B, and an A-B bond, with all the two-chain molecules of  $\beta$ -A and  $\beta$ -B being capable of participating in the reaction. The difference in the free energies of these bonds is due to a difference in entropy which, in turn, may reflect the substitution of an aspartic acid residue in  $\beta$ -A for a glycine in  $\beta$ -B.<sup>9</sup> The full significance of the thermodynamic parameters reported here as well as previously will be discussed in a subsequent publication.

**Acknowledgment.** The authors wish to thank Dr. Robert Townend for many interesting discussions and valuable suggestions in the course of this work.

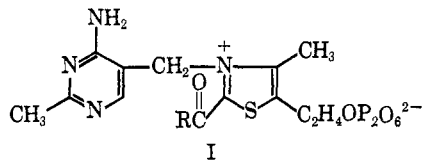
## Kinetics and Mechanism of the Hydrolysis of 2-Acetyl-3,4-dimethylthiazolium Ion<sup>1</sup>

Gustav E. Lienhard

Contribution from the James Bryant Conant Laboratory, Harvard University, Cambridge, Massachusetts 02138. Received July 27, 1966

**Abstract:** 2-Acetyl-3,4-dimethylthiazolium ion in aqueous solution undergoes rapid, general base catalyzed hydration to yield 2-(1,1-dihydroxyethyl)-3,4-dimethylthiazolium ion. At 25° at equilibrium there are approximately equal amounts of the unhydrated and hydrated compounds. 2-(1,1-Dihydroxyethyl)-3,4-dimethylthiazolium ion is stable in acid, but under more basic conditions cleaves to acetic acid and dimethylthiazolium ion in a reaction that occurs by specific hydroxide ion catalysis. Thiols and phosphate dianion, but not imidazole, appear to form carbonyl adducts with 2-acetyl-3,4-dimethylthiazolium ion. Transfer of the acetyl group from 2-acetyl-3,4-dimethylthiazolium ion to thiols, phosphate, and imidazole does not occur to any significant extent in water. The relevance of these findings to the role of thiamine in enzymatic reactions is discussed.

The 2-acylthiamine pyrophosphates (I) have been proposed as intermediates in several thiamine pyrophosphate-dependent enzymatic reactions. These



include the phosphoketolase reaction, in which 2-acetylthiamine pyrophosphate may form from several hydroxymethyl ketone substrates and undergo phosphorolysis to yield acetyl phosphate,<sup>2-4</sup> and the reac-

tions catalyzed by the pyruvate and  $\alpha$ -ketoglutarate dehydrogenation complexes, in which 2-acetyl- and 2-succinylthiamine pyrophosphate or at least their corresponding hemithioketals are probably intermediates in the formation of S-acetyl- and S-succinyl-dihydroxy-lipoic acid from 2-(1-hydroxyethyl)- and 2-(1-hydroxy-3-carboxypropyl)thiamine pyrophosphate and oxidized lipoic acid.<sup>3,5,6</sup> In addition, the oxidation of several 2-(1-hydroxyalkyl)thiamine pyrophosphate compounds by artificial electron acceptors such as 2,6-dichlorophenol, indophenol, and ferricyanide is catalyzed by phosphoketolase,<sup>7</sup> the pyruvate and  $\alpha$ -ketoglutarate dehydrogenation complexes,<sup>8</sup> an acetoin-

(1) Supported by a grant (GB 4848) from the National Science Foundation.

(2) R. Breslow, *J. Cellular Comp. Physiol.*, **54** (Suppl 1), 100 (1959).

(3) F. G. White and L. L. Ingraham, *J. Am. Chem. Soc.*, **84**, 3109 (1962).

(4) M. L. Goldberg and E. Racker, *J. Biol. Chem.*, **237**, PC 3841 (1962).

(5) M. L. Das, M. Koike, and L. J. Reed, *Proc. Natl. Acad. Sci., U. S.*, **47**, 753 (1961).

(6) D. R. Sanadi, *Enzymes*, **7**, 307 (1963).

(7) W. Schröter and H. Holzer, *Biochem. Biophys. Acta*, **77**, 474 (1963).

(8) F. da Fonseca-Wollheim, K. W. Bock, and H. Holzer, *Biophys. Biochem. Res. Commun.*, **9**, 466 (1962).